

Tracking Targets with Quality in Wireless Sensor Networks

Guanghai He and Jennifer C. Hou
Univ. of Illinois at Urbana Champaign
Urbana, Illinois 61801
{ghe,jhou}@cs.uiuc.edu

Abstract

Tracking of moving targets has attracted more and more attention due to its importance in utilizing sensor networks for surveillance. In this paper, we consider the issue of how to track mobile targets with certain level of quality of monitoring (QoM), while conserving power. We address the target tracking problem by taking into account of both the coverage and the QoM. In particular, QoM ensures that the probability of reporting inaccurate monitoring information (such as false alarm or target miss) should be as small as possible, even in the presence of noises and signal attenuation. We also analytically whether or not the detection/observation made by a single sensor suffices to tracking the target in a reasonably populated sensor network. Our finding gives a confirmative answer and challenges the long-held paradigm that high tracking quality (low tracking error) necessarily requires high power consumption.

To rigorously analyze the impact of target movement on QoM, we derive both lower and upper bounds on the number of sensors (called duty sensors) required to keep track of a moving target. Based on the analysis, we have devised a cooperative, relay-area-based scheme that determines which sensor should become the next duty sensor when the target is moving. The simulation study indicates that the number of duty sensor required in the proposed scheme is, in the worst case, approximately 1.2 times larger than the lower bound. It also indicates that a trade-off exists among QoM, the number of duty sensors required, and the load balance.

1 Introduction

Use of wireless networks of unattended sensor devices for intelligence gathering and environmental monitoring [5, 1, 11] has become an emerging trend recently. Among several potential applications, tracking of mobile targets has attracted considerable attention in the literature, and has found its application in monitoring wildlife animals, vehicles on the freeway, and surveilling troops in the battle field.

Prior work on tracking moving targets [23, 26, 8, 30, 31, 32] focuses on enabling sensor nodes to cover the area in which the target moves and coordinating sensor nodes in the vicinity of the target to determine the target location. A plausible assumption has been made that as long as the target is within the sensing range of a sensor, it can be detected. In reality, this assumption may not always hold true. Even if a target is within the sensing range of a sensor, the decision made by the sensor may not be accurate due to signal attenuation and noises. Coverage should not be the only

criterion in devising target tracking application; instead, the quality of monitoring (which takes into account of signal attenuation and noises) has to be considered.

Another dimension of complexity in tracking moving targets is the power incurred in tracking targets. As power is always a valuable and non-replenishable resource in sensor networks, it has been advocated that only a small subset of sensor nodes is powered on for the purpose of surveillance and tracking. For example, Patten *et al.* [17] have proposed four schemes: naive activation, randomized activation, selective activation based on trajectory prediction and duty-cycled activation. Work also exists that enables a small subset of sensor nodes to power on for the sake of coverage and connectivity, e.g., ASCENT [6] and PEAS [28], CCP [24], and OGDC [29]. The common belief is that all the power management schemes trade the quality of tracking for energy saving. In particular, a target may be missed because some of the sensors in the vicinity of a target operate in the power-saving mode and hence cannot provide adequate information. In reality again this belief may not be always true, because in a reasonably-populated sensor network, one observation made by a sensor in the vicinity of the target detecting both the existence and position of the target may suffice.

In this paper, we consider the issue of tracking mobile targets with certain level of *quality of monitoring* (QoM), while conserving power. We address the target tracking problem by taking into account of both the *coverage* and the *QoM*. By *coverage*, we mean that during the movement of a target, the target is covered with high probability, while by *QoM* we mean a certain level of confidence in monitoring a target, i.e., the probability of reporting inaccurate monitoring information (such as false alarm or target miss) is as small as possible. We also study analytically the issue of whether or not the detection/observation made by a single sensor suffices to tracking the target in a reasonably populated sensor network. As will be elaborated on in Section 3.3, *our findings challenge the long-held paradigm that high tracking quality (low tracking error) necessarily requires high power consumption.*

To rigorously analyze the impact of target movement on QoM, we derive both the lower and upper bounds on the number of sensors (called *duty sensors*) required to keep track of a moving target. Based on the analysis, we then devise a cooperative, *relay-area-based* scheme that determines which sensor should become the next duty sensor when the target is moving. The scheme is designed with three objectives: first, the moving target should be covered with predefined QoM; second, the number of *duty sensors* should be as close to the derived lower bound as possible; third, the energy consumed in target tracking should be kept as small as possible. Although the first objective conflicts with the latter two, a trade-off is made based

on the analytical results. The simulation result indicates that the number of *duty sensor* required in the proposed scheme is, in the worst case, approximately 1.2 times larger than the lower bound.

The rest of the paper is organized as follows. In Section 2 we briefly summarize existing work on target tracking. In Section 3 we give a formal definition of quality of monitoring (QoM). Following that, we study in Section 4 the issue of whether or not the detection/observation made by a single sensor suffices to tracking targets, with respect to the node density of the network. The effect of target movement on QoM is discussed in Section 4. In particular, we derive both lower and upper bounds on the number of duty sensors required to accurately keep track of a moving target. Based on the derivation, we then propose in Section 5, a cooperative, *relay-area-based* scheme that designates the next duty sensor(s) in the course of target moving, with the objective of maintaining a pre-specified QoM, while keeping the number of duty sensors as close to the derived lower bound as possible. We evaluate the proposed scheme via simulation in Section 6 and conclude the paper in Section 7.

2 Related Work

2.1 Research on Tracking Moving Targets

Tracking moving targets in large scale sensor networks has gained extensive attention recently. Both Chu *et al.* [10] and Zhao *et al.* [32] propose *leader-based* target tracking schemes that enable sensor nodes to track targets, based on optimizing the information utility of data, given the cost of communication and computation. As the hand-off operation (of designating the next leader) is carried out on an one-on-one basis, the scheme is susceptible to control message losses and may not be robust.

Based on the minimalist binary sensor model, Aslam *et al.* [2] and Mechitov *et al.* [16] propose several tracking schemes. Each sensor's value is converted reliably to one bit of information: whether the object is moving toward the sensor or away from the sensor, and the tracking scheme is then designed based on the information. As stated in [2, 16], these schemes do not explicitly take into account of the quality of the received signals.

Wang *et al.* [23], Chen *et al.* [8], and Yang and Sikdar [26] propose cluster-based tracking schemes. They envision a hierarchical sensor network that is composed of (a) a static backbone of sparsely placed high-capability sensors which will assume the role of a cluster head (CH) upon triggered by certain signal events; and (b) moderately to densely populated low-end sensors whose function is to provide sensor information to CHs upon request. In these schemes, sensors are grouped into clusters either statically or dynamically (upon detection of the target in the vicinity), and a cluster-head collects information from its cluster members and determines the target location using either the trilateration technique [23] or the Voronoi diagram-based approach [8]. Both localization approaches aim to determine the exact location of the target at the expense of considerable computational overhead.

Zhang and Cao [30, 31] introduce tree-based tracking approaches, in which the notion of dynamic convoy tree-based collaboration is defined and the tracking problem is formalized as a multiple objective optimization problem. The solution to the problem is a convoy tree sequence with high tree coverage and low energy consumption. Building such a convoy tree sequence requires global network information, and re-configuration and maintenance

of a convoy tree incurs considerable computational and communication overhead. As a result, the tree-based approaches are usually centralized and applied in the deployment phase of sensor networks.

A study on power-centric sensor deployment schemes that are independent of tracking methods and collaboration protocols is performed in [12]. The notion of quality of surveillance is introduced and used to guide the protocol design. The quality of monitoring a target (in terms of the confidence in determining the existence of a target) is not considered.

2.2 Research on Ensuring Network Coverage

As mentioned in Section 1, coverage is one of the two criteria in characterizing the quality of target tracking. A detailed survey on the coverage models and solutions is provided in [4]. Approximation-based or integer-programming-based techniques are widely used to determine the minimum set of nodes for covering the entire monitoring area [4, 21, 7]. The resulting schemes are usually centralized, as they require availability of global network information.

Coverage is usually considered in conjunction with connectivity (but not with QoM). Both Wang *et al.* [24] and Zhang and Hou [29] study the fundamental relationship of sensing coverage and communication connectivity. Wang *et al.* prove that coverage infers connectivity if the radio range is at least twice of the sensing range, and that if all the crossing points inside a region (or disk) are covered then the region (or disk) is covered. They then devise the *coverage and configuration protocol* (CCP), in which each node collects neighboring information and then use this as an eligibility rule to decide if it can sleep. In the case that the radio range is less than twice of sensing range, they combine their protocol with SPAN [9] to form a connected covering set. Zhang and Hou, on the other hand, intend to find the *minimal* number of sensors that maintain coverage and connectivity. They devise an *optimal geographical density control* (OGDC) algorithm, based on the optimization analysis.

Huang and Tseng [15] lay a foundation for testing network *p-coverage* solely based on local information. The solution is grounded on the assertion that if every location of the field is covered by at least p sensors then the network is p -coverage.

3 Quality of Monitoring

In this section we first state the assumptions made throughout the paper and formally define QoM. Then we study the issue of whether or not it suffices to using the observation made by the sensor that is closest to a target to determine the existence of the target. It is intuitive that if the sensor network is densely populated, then the closest-sensor-based approach may suffice. An interesting question is then under what condition (e.g., the minimum nodal density required) this simple approach is able to achieve a certain level of QoM.

3.1 Systems Model

We assume that sensors are uniformly and randomly distributed according to a Poisson point process with the node density λ (this assumption is relaxed for performance evaluation in Section 6). There are several ways of defining a Poisson point process, one of which is stated below. First, for any subset A of the region R , the

distribution of the number of nodes in the set is Poisson with mean $\lambda||A||$, where $||A||$ is the area of A . Second, given that the number of nodes in such a set A is m , the node locations in A are m mutually independent random variables, each uniformly distributed over A . It is well known that n nodes whose locations are mutually independent random variables, each with uniform distribution in R , are essentially a Poisson point process with density $\lambda = n/\ell^2$ if R is large ([13], page 39).

We also assume that each sensor node has the capability to gather its own location information via, for example, *pseudolite* for indoor applications and other lightweight localization techniques for wireless networks (the interested reader is referred to, for example, [14] for a summary).

3.2 The Distance Between a Target and its Closest Sensor

For any position P_t in the monitoring area, let D be the distance between P_t and the sensor that is closest to P_t . Under the assumption of a Poisson point process, D is a random variable and its probability density function (pdf) of D can be expressed as

$$f_D(d) = 2\pi\lambda e^{-\pi d^2\lambda}, \quad d \geq 0. \quad (1)$$

It then follows that the expectation value of D is $E(D) = \frac{1}{2\sqrt{\lambda}}$ and the standard deviation of D is $S(D) = \sqrt{\frac{1}{\lambda}\sqrt{\frac{1}{\pi} - \frac{1}{4}}}$. Theoretically, the value of D can go to infinity for any finite λ . However, the complementary cumulative distribution function (CCDF) of D decreases in an exponential manner with D , especially for large λ , i.e.,

$$\Pr(D \geq x) = \exp^{-\pi\lambda x^2}. \quad (2)$$

For example, it is easy to check that when $\lambda = 1$ (i.e., one sensor node per unit square area) and D is as large as $E(D) + 4 \times S(D)$, the CCDF is as small as 0.0056. In fact, one can show that when the nodal density $\lambda \geq 1$ the closest sensor is within the distance of

$$\tilde{D} = \frac{1}{\sqrt{\lambda}}\left(\frac{1}{2} + 4\sqrt{\frac{1}{\pi} - \frac{1}{4}}\right), \quad (3)$$

with high probability ($\geq 99\%$).

In summary, for any position in the monitoring area, with high probability ($\geq 99\%$) at least one sensor exists within the distance of \tilde{D} as long as $\lambda \geq 1$. (Note that \tilde{D} is a function of λ .) With this observation, the next question is then, whether or not we can use the observation made by the closest sensor to a target for target tracking, and if so, what is the level of confidence in determining the existence of the target. To answer this question, we first define QoM in the next subsection.

3.3 Definition of QoM

As mentioned in Section 1, in the presence of noises and signal attenuation, the signal sensed by a sensor may be ‘‘polluted,’’ and leads to erroneous detection, even if the target is within the sensing range of the sensor. In other words, it is not sufficient to use coverage as the only criterion for target tracking. Instead, one should take into account of the received signal strength and the associated noise in determining the quality of monitoring and tracking. Specifically, let the false alarm probability, P_F , be the probability of making a

positive assertion in the absence of a target, and the missing probability, P_M , the probability of declaring no target when there is one. Then, we define QoM as follows.

Definition 1 ($QoM(\alpha, \beta)$) *A target located at (x, y) is said to be monitored with $QoM - (\alpha, \beta)$, if it can be detected with*

$$P_F \leq \alpha, \quad (4)$$

and

$$P_M \leq \beta. \quad (5)$$

To figure in the physical layer characteristics, we introduce the likelihood-based detection model and the signal attenuation model.

Detection Model A sensor determines whether or not a target is present based on its sensed signal z . The task of determining the presence/absence of a target is then to test the following two hypotheses:

$$H^0 : \text{with pdf } p(z|H^0), \quad (6)$$

$$H^1 : \text{with pdf } p(z|H^1), \quad (7)$$

where $p(z|H^0)$ follows a Gaussian distribution with zero mean, i.e., the signal strength that a sensor senses in the absence of a target is simply the background noise:

$$p(z|H^0) = \frac{1}{\sqrt{2\pi}\sigma} \exp\left(-\frac{z^2}{2\sigma^2}\right) \quad (8)$$

and

$$p(z|H^1) = \frac{1}{\sqrt{2\pi}\sigma} \exp\left(-\frac{(z - \sqrt{a(x', y')})^2}{2\sigma^2}\right), \quad (9)$$

where $a(x', y')$ is the average power sensed by a sensor located at (x', y') . (The expression of $a(x', y')$ will be given below in Eq. (11).) Finally, the likelihood ratio is defined as

$$\Lambda(z) = \frac{p(z|H^1)}{p(z|H^0)}. \quad (10)$$

Signal Attenuation Model In spite of the fact that sensing devices generally have widely different physical characteristics, they usually share one feature in common: their sensing ability diminishes as the distance to the target increases. For example, an acoustic sensor detects the target by sensing the amplitude of the sound signal, which attenuates in proportion of the distance from the target. Specifically, given a target located at (x, y) , the signal strength received by a sensor located at (x', y') can be expressed as

$$a(x', y') = \frac{a_0}{d((x, y), (x', y'))^m}, \quad (11)$$

where d denotes the Euclidean distance between two points, a_0 is the initial power of the signal emitted by the target, and m is the attenuation factor determined by the physical characteristics of the signal. Usually $2 \leq m \leq 4$.

3.4 Target Tracking with the Use of the Closest Sensor

Given the definition of QoM, we are now in a position to investigate whether or not the observation made by the sensor that is closest to a target is sufficient to meet the $QoM(\alpha, \beta)$ (with pre-specified α and β) in a network with the node density λ . In Section 3.2, we have shown that as long as $\lambda \geq 1$, the distance between a target and the closest sensor is within $[0, \tilde{D}]$ with high probability, where \tilde{D} is defined in Eq. (3). In this subsection, we investigate whether or not $QoM(\alpha, \beta)$ can be met by only considering the observation made by the closest sensor based on its received signal strength y .

By hypothesis testing, a sensor with the received signal y makes the following decision:

$$\Lambda(z) \geq \eta_1, \text{ decide that } H^1 \text{ is true,} \quad (12)$$

$$\Lambda(z) \leq \eta_0, \text{ decide that } H^0 \text{ is true,} \quad (13)$$

where in order for $P_F = \alpha$ and $P_M = \beta$ to hold true, η_0 and η_1 should satisfy [22]

$$\eta_1 = \frac{1 - \beta}{\alpha}, \quad (14)$$

and

$$\eta_0 = \frac{\beta}{1 - \alpha}. \quad (15)$$

To check whether or not $QoM(\alpha, \beta)$ can be met, we need to derive $\Pr(\Lambda(z) \geq \eta_1 \mid \text{existence of a target})$ and $\Pr(\Lambda(z) \leq \eta_0 \mid \text{the absence of targets})$. With the definitions in Eq. (8) and Eq. (9) we have

$$\log(\Lambda(z)) = \frac{1}{\sigma^2} \left(z \sqrt{\frac{a_0}{d((x, y), (x', y'))^m}} - \frac{a_0}{2d((x, y), (x', y'))^m} \right). \quad (16)$$

For notational convenience, we use d to denote $d((x, y), (x', y'))$. After several algebraic operations, we have that in order for $\Lambda(z) \geq \eta_1$ or $\Lambda(z) \leq \eta_0$ to hold true, the following condition must hold

$$\frac{z}{\sigma} \geq \frac{\log(\eta_1)\sigma}{\sqrt{\frac{a_0}{d^m}}} + \frac{\sqrt{\frac{a_0}{d^m}}}{2\sigma}, \quad (17)$$

or

$$\frac{z}{\sigma} \leq \frac{\log(\eta_0)\sigma}{\sqrt{\frac{a_0}{d^m}}} + \frac{\sqrt{\frac{a_0}{d^m}}}{2\sigma}. \quad (18)$$

Given $\alpha = \beta$, we have $\log(\eta_1) = -\log(\eta_0)$, and

$$\begin{aligned} \tilde{P} &\triangleq \Pr(\Lambda(z) \geq \eta_1 \mid H^1) = \Pr(\Lambda(z) \leq \eta_0 \mid H^0) \\ &= \begin{cases} \frac{1}{2} + \text{erf}\left(\left|\frac{\log(\eta_1)\sigma}{\sqrt{\frac{a_0}{d^m}}} - \frac{\sqrt{\frac{a_0}{d^m}}}{2\sigma}\right|\right), & \text{if } \left|\frac{\log(\eta_1)\sigma}{\sqrt{\frac{a_0}{d^m}}}\right| > \left|\frac{\sqrt{\frac{a_0}{d^m}}}{2\sigma}\right|, \\ \frac{1}{2} - \text{erf}\left(\left|\frac{\log(\eta_1)\sigma}{\sqrt{\frac{a_0}{d^m}}} - \frac{\sqrt{\frac{a_0}{d^m}}}{2\sigma}\right|\right), & \text{if } \left|\frac{\log(\eta_1)\sigma}{\sqrt{\frac{a_0}{d^m}}}\right| \leq \left|\frac{\sqrt{\frac{a_0}{d^m}}}{2\sigma}\right|, \end{cases} \end{aligned} \quad (19)$$

where $\text{erf}(x) = \int_0^x \frac{1}{\sqrt{2\pi}} \exp(-t^2/2) dt$, is the error function of *normal* distribution $N(0, 1)$. In general, a high level of QoM requires both α and β be small. As it is reasonable to make the assumption that $\alpha = \beta$, we only need to calculate either one of the two values in Eq. (19).

Fig. 1 (a) depicts \tilde{P} as a function of the node density λ and the distance d for $QoM(\alpha = 0.05, \beta = 0.05)$. The relationship between λ and \tilde{D} is shown in Fig. 1 (b). (The initial signal strength and the variance of the white noise are set to $a_0 = 200$ and $\sigma^2 = 1$.) As shown in Fig. 1, when the nodal density $\lambda \geq 1$ and $d \leq \tilde{D}$, \tilde{P} is

very close to 1. Another observation is that the QoM decreases as d increases.

The important implication in Fig. 1 is that for a reasonably densely populated sensor network, as long as the target is within distance \tilde{D} of a sensor, $QoM(\alpha, \beta)$ can be met with high probability (≈ 1). For this reason, we term \tilde{D} the *virtual sensing range*.

4 Impact of Mobility on QoM of Target Tracking

In this section, we study the impact of mobility on the QoM, i.e., when a target moves in compliance with certain mobility model, what is the percentage of the target trace that can be “covered” by sensors. By “covered,” we mean the area is within the *virtual sensing range* of certain sensors. Alternatively, we can derive the minimum number of sensors required to cover the entire trace. For ease of analysis, we assume that a target follows the random waypoint model [3, 19]. However, we claim that the notion of QoM and the analysis methodology can be applied to other mobility models.

Specifically, in the random waypoint model, a node randomly chooses a destination point in the area and moves at a constant speed toward it. After the node arrives at the destination point, it pauses for a random time, chooses a new destination, and moves toward that destination. A major feature of the random waypoint model is that the trace of the moving target consists of line segments. We first study the coverage of a line segment, and derive an upper bound and an lower bound on the number of sensors needed to cover a segment of length ℓ . We call the sensors that are required to be active in order to cover the segment *duty sensors*. Then we extend the results to a concatenation of line segments.

4.1 Average Number of Duty Sensors Required to Cover a Line Segment

The covered monitoring area consists of a set of discs $C = \{x_i + U, 1 \leq i \leq N\}$, where x_i is the location of sensor i and U is the disk with radius \tilde{D} and centered at the origin. We first derive the average length of the portion of a line segment that is contained in a covering disk. We term this portion of line segment the *chord*.

Average length of the chord Given that a line segment intersects with a covering disk, the distance from a sensor to the line segment, d_x , follows the uniform distribution in $[0, \tilde{D}]$. The probability density function (pdf) of the length of the chord ℓ_i can be expressed as

$$f_{\ell_i} = \frac{1}{4\tilde{D}} \cdot \frac{\ell}{\sqrt{\tilde{D}^2 - \frac{\ell^2}{4}}}, \ell \in [0, 2\tilde{D}], \quad (20)$$

and hence the expectation of the chord ℓ_i is

$$E(\ell_i) = \tilde{D} \cdot \frac{\pi}{2}. \quad (21)$$

That is, on average, the length of a chord (the portion of a line segment covered by a covering disk) is $\tilde{D} \cdot \frac{\pi}{2}$. If the covering disks do not overlap, the average number of duty sensors needed to cover a line segment of length L is $\lceil \frac{2L}{\pi\tilde{D}} \rceil$. In reality, however, with high likelihood covering disks overlap, and $\lceil \frac{2L}{\pi\tilde{D}} \rceil$ serves as a lower bound.

To derive the upper bound, we leverage a direct extension of Theorem 4.3 in [13]:

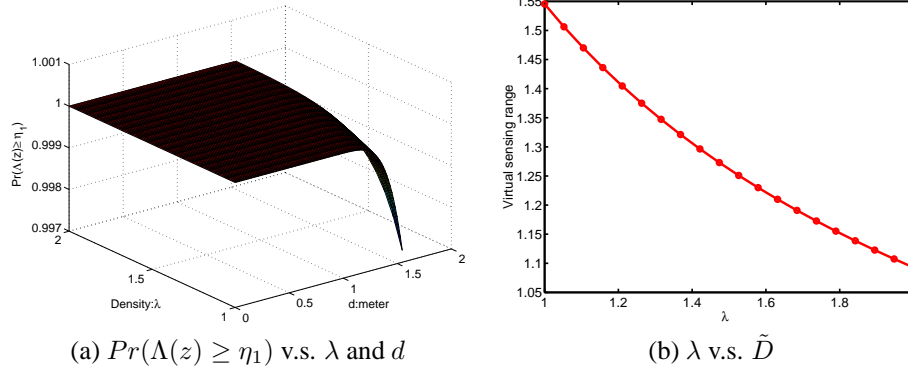


Figure 1. The probability that the likelihood function is greater than or equal to the threshold and the relation between \tilde{D} and λ .

Theorem 1 For a segment with length L , the expected number of intersections of the segment with the boundaries of covering discs is $4\lambda \cdot L \cdot \tilde{D}$.

Since a line segment intersects a disk at either one or two points, we have $2\lambda \cdot L\tilde{D} \leq N_e \leq 4\lambda \cdot L\tilde{D}$. Hence, the average number of sensors N_e needed to cover a segment of length L follows

$$\left\lceil \frac{2L}{\pi\tilde{D}} \right\rceil \leq N_e \leq \lceil 4\lambda \cdot L\tilde{D} \rceil. \quad (22)$$

Two points are in order. First, the above upper bound is derived based on the condition that the area is covered by sensors with the virtual sensing range \tilde{D} ; Second, the underlying assumption in the above analysis is that the nodal density is sufficiently high so that the entire area is covered. Shakkottai *et al.* [20] have shown that as long as $\pi\lambda D^2 \geq \log \lambda + [\phi(\lambda) + \log \log \lambda]$, where $\phi(x)$ is a slowly-growing function and D is the sensing range of a sensor, the entire area is covered by the covering discs. We assume that the initial sensor deployment meets the requirement of the above condition.

In summary, in order to cover a line segment of length L , the number of duty sensors required satisfies Eq. (22). One interesting observation is that the upper bound of N_e is proportional to \tilde{D} while the lower bound of N_e is inverse proportional to that.

4.2 Average Number of Duty Sensors Required to Cover the Entire Trace

In this subsection, we derive the average number of duty sensors required to cover the entire trace. We first study the distribution of the direction taken by a target in the random waypoint model (which we will leverage in the analysis) and then analyze how mobility affects the average number, N_e , of *duty sensors*.

4.2.1 Direction of RWP in a grid

As indicated in [12], direction changes will affect the length of the chord (that can be covered by a covering disk) in a complicated manner. In our derivation, we find that the direction taken by a target is not uniformly distributed around the target in a square area, but instead depends on the current location of the target in the field. A detailed derivation on the probability density function of the direction of a moving target is given in Appendix A. The failure of the

direction (taken by a target) to conform to the uniform distribution precludes us from extending results in Section 4.1 in a straightforward manner.

4.2.2 Average length of the trace covered by a covering disk

Let ℓ_c be defined as the length of the target trace that is covered by a duty sensor before the target moves out of the virtual sensing range. Let (x_s, y_s) and (x_t, y_t) be, respectively, the position of the sensor that is on duty and the position of the target. Obviously, ℓ_c is a function of $\{x_t, y_t, x_s, y_s\}$. We first find the expression for ℓ_c given these parameters, and then derive its statistic property (mean).

For ease of analysis, we ignore the boundary effect (which diminishes as the ratio of a to \tilde{D} grows large). As shown in Fig. 2, we divide the entire area into four regions (four triangles). Given the position of the target (x_t, y_t) , the duty sensor can be in any one of the four regions. We also define the four angles, α , β , γ , and θ as shown in Fig. 2. In particular, α , β , and γ are defined based on line ℓ —the line that is perpendicular to the line connecting the target and the duty sensor, and γ specifies the moving direction. With all the definitions, it is straightforward to obtain that $\theta = \arctan(\frac{y_s - y_t}{x_s - x_t}) - \arctan(\frac{y_t + a}{x_t + a})$, $\beta = \pi/2 - \theta$ and $\alpha = \pi/2 - \arctan(\frac{y_s - y_t}{x_s - x_t}) - \arctan(\frac{y_t + a}{x_t + a})$.

Given the position of the target (x_t, y_t) and the current duty sensor (x_s, y_s) (and hence θ), the length of the target trace covered by a duty sensor $\ell_c(x_t, y_t, \theta)$ can be expressed as

$$\ell_c(x_t, y_t, \theta) = 2\tilde{D} \cdot \sin(\gamma), \quad (23)$$

where γ is a random variable, and for any given $\{x_t, y_t, \theta\}$ it changes from 0 to 2π . Let $f(\gamma|x_t, y_t, \theta)$ be the conditional pdf of γ , which is given in Appendix Eq. (29) (as γ can be expressed in terms of δ). Hence we have the conditional mean

$$\bar{\ell}_c(x_t, y_t, \theta) = \int_0^{2\pi} 2\tilde{D} \cdot \sin(\gamma) \cdot f(\gamma|x_t, y_t, \theta) d\gamma, \quad (24)$$

$$\bar{\ell}_c(x_t, y_t) = \int_0^{2\pi} \int_0^{2\pi} 2\tilde{D} \cdot \sin(\gamma) \cdot f(\gamma|x_t, y_t, \theta) d\gamma d\theta \quad (25)$$

and,

$$\bar{\ell}_c = \int_{-a}^a \int_{-a}^a \int_0^{2\pi} \bar{\ell}_c(x_t, y_t, \theta) dx_t dy_t d\theta$$

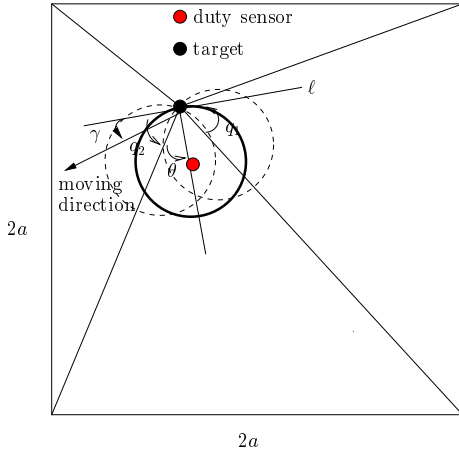


Figure 2. Four regions and *regime-circle*.

$$= \int_{-a}^a \int_{-a}^a \int_0^{2\pi} \int_0^{2\pi} 2\tilde{D} \cdot \sin(\gamma) \cdot f(\gamma|x_t, y_t, \theta) d\gamma dx_t dy_t d\theta. \quad (26)$$

Figure 3 depicts $\bar{\ell}_c(x_t, y_t)$ in the case that $\tilde{D} = 5$. Once a target enters the sensing region of a sensor with the virtual sensing radius \tilde{D} , on average it can travel a distance of $\bar{\ell}_c$ and still under the surveillance of the current sensor. Two observations are in order: first, as shown in both figures, ℓ_c is susceptible to both the target position and the moving direction. Second, from Fig. 3, we obtain $\bar{\ell}_c = 5.4851 \approx 1.1 \cdot \tilde{D}$. Since $\bar{\ell}_c$ is proportional to \tilde{D} by Eq. (26), the coefficient 1.1 is applicable to all the configurations. Note that in the case that a target may change its direction according to the RWP model, the chord $\bar{\ell}_c$ is smaller. The lower bound on the number of *duty sensors* required to cover a line segment of length L (Eq. (22)) can then be refined as

$$\lceil \frac{L}{1.1\tilde{D}} \rceil \leq N_e \leq \lceil 4\lambda L\tilde{D} \rceil. \quad (27)$$

Note that the upper bound in Eq. (27) is the same as that in Eq. (22). This is because Theorem 1 still holds when there are direction changes.

In the next section, we will leverage the above result (Eq.(27)) and devise a cooperative, *relay-area-based* target tracking algorithm that determines which sensor should act as a *duty sensor*, with the objective of (approximately) achieving the lower bound.

5 A Cooperative, Relay-Area-Based Hand-Off Scheme

In Section 4, we have derived the average length of the target trace that can be covered by a duty sensor, and the lower bound on the number of *duty sensors* required to cover a straight target trace of length L . In this section, we devise a *relay-area-based* hand-off scheme that determines in a decentralized manner which sensor(s) should enter the tracking mode and act as duty sensors, as the target moves. The objective is to approach the lower bound on the number of duty sensors required.

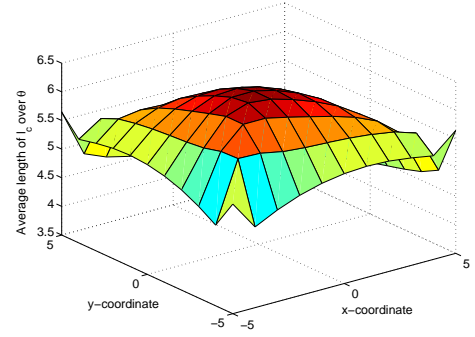


Figure 3. The average length of the target trace covered by a duty sensor $\bar{\ell}_c(x_t, y_t)$, in the case that \tilde{D} .

5.1 Detailed Description of the Relay-Area-Based Scheme

The proposed scheme operates as follows: when a target appears, the sensor that detects the existence of the target will broadcast, after a random delay, a short *on-duty* message expressing its willingness to be a duty sensor. The random delay is determined based on the received signal strength, and if the sensor receives a broadcast *on-duty* message from some other sensor before its own broadcast, it suppresses its own broadcast and will not be a duty sensor. Once a sensor broadcasts the message, it becomes a duty sensor.

After a sensor becomes a duty sensor, it continuously monitors the target movement and determines the moving direction of the target based on the angles-of-arrival of consecutive measurements. With the knowledge of its own position¹ and its virtual sensing range (\tilde{D}), the duty sensor can determine the position P_o at which the target moves out of its covering area (Fig. 4). Before the target approaches the position P_o , the sensor broadcasts a *relay* message that includes (i) the direction of the target (expressed in the slope of the moving line with respect to a reference system agreed upon by all the sensors), (ii) the position P_o , and (iii) the *relay area* in which the next duty sensor will be selected. As shown in Fig. 4, the *relay area* is defined by three tunable parameters: ϕ , \tilde{D} and the width w_r . With the three parameters, the size of the *relay area* is $\frac{\phi}{2}(2\tilde{D}w_r - w_r^2)$.

How to appropriately set the three parameters depends on the node density λ . In general one should ensure that the relay area is properly sized so that at least one sensor lies in it. Under the assumption of a Poisson point process, the probability that no sensor exists in the relay area is $P_{null} = \exp(-\lambda \cdot \frac{\phi}{2}(2\tilde{D}w_r - w_r^2))$. Fig. 5 depicts P_{null} when $\tilde{D} = 1$, $\lambda = 0.5$, w_r changes from $0.5\tilde{D}$ to \tilde{D} , and ϕ changes from 0.4π to π . As shown in Fig. 5, as long as the nodal density is reasonably high, small values of ϕ and w_r can be chosen to narrow the scope of searching for candidates for the relay process.

As illustrated in Fig. 4, one of the the key results that the *relay-area-based* hand-off scheme leverages is that the next duty sensor is, if possible, located \tilde{D} distance away from P_o along the moving target direction. This will reduce the degree of overlapping in the covering disks between consecutive duty nodes.

¹Recall that in Section 3.1, we make the assumption that each sensor node knows its own position.

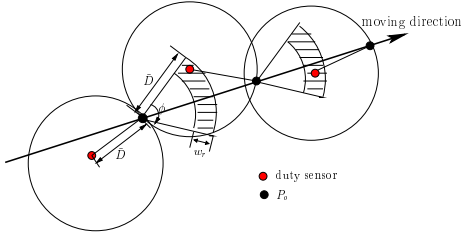


Figure 4. An illustration that shows how the current duty node determines the relay area. All the parameters needed to define the relay area are given in the figure.

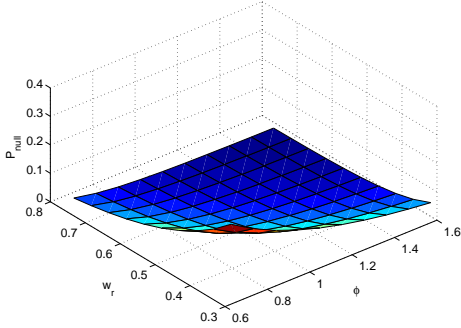


Figure 5. The probability, P_{null} , that there exists no sensor node in a relay area as a function of w_r and ϕ .

Upon receiving the *relay* message from a duty sensor, each sensor can determine whether or not it lies in the relay area, based on the information contained in the relay message and its own position. If the sensor is located in the relay area, it calculates its distance to the line of the moving direction, d_m and the distance to P_o , d_{P_o} . Then, the sensor sets up a timer with the timeout value $t_o \propto \frac{d_m}{d_{P_o}}$, and broadcasts a *duty* message upon timeout. The timer is suppressed if a broadcast message is received from some other sensor. This gives the largest likelihood that the sensor that is most distance from P_o and closest to the line of the moving direction will become the next *duty sensor*. In this manner, the overlap in the covering areas between consecutive *duty sensors* can be reduced and the lower bound of N_e can be approximately achieved.

A duty sensor has three tasks: (1) it continuously monitors the moving target and determines the moving direction of the target; in case that the moving target changes its direction in the covering disk of the duty sensor, it determines the new position, P_o , at which the moving target will leave its covering disk; (2) it broadcasts a *relay* message to inform candidate duty sensors along the target moving direction, when the target approaches P_o ; and (3) it relays the tracking and monitoring information to interested subscribers.

5.2 Scheme Refinement in the Case That a Target Changes the Direction Right After the Hand-Off

For clarity of explanation, in Section 5.1, we did not consider the (rare) case that right after the moving target moves out of the current

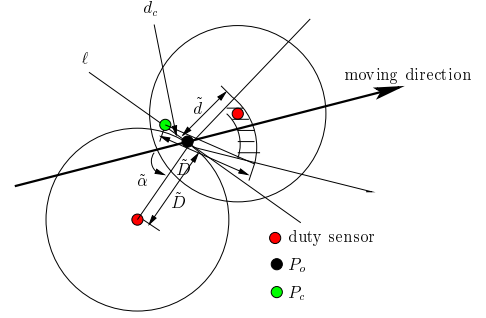


Figure 6. An illustration that shows how the direction change right after a hand-off may affect the relay area. All the parameters needed to define the relay area are given in the figure.

covering disk, it changes its direction and moves toward some other direction. To deal with this case, we have to shorten the distance between P_o and the relay area (originally set to \tilde{D}) in the scheme as follows. As shown in Fig. 6, without loss of generality, we divide the entire region into two parts with line ℓ . Note that line ℓ is perpendicular to the line connecting P_o and the current duty sensor. If the direction change takes place on the left hand side of line ℓ , it can be detected by the current duty sensor and a new position P_o and the corresponding relay area can be determined.

On the other hand, if the direction change takes place on the right hand side of line ℓ , the next duty sensor should be responsible for any necessary adjustment. Let the new distance between the position P_o and the relay area be denoted as \tilde{d} . As the extreme case occurs when the target moves upward along line ℓ right after the hand-off, it is easy to observe from Fig. 6 that, as long as $\tilde{d} \leq \tilde{D}$, the new duty sensor is still capable of determining the new moving direction. The value of \tilde{d} is determined by (i) the angle of the cone ϕ , (ii) the virtual sensing range \tilde{D} , (iii) the angle, $\tilde{\alpha}$, between the original moving direction and the line connecting P_o and the current duty sensor, and (iv) the distance, d_c , that a target can move upward along line ℓ before a new duty node in the current relay area fails to detect the target (i.e., the distance between P_o and P_c in Fig. 6). It is straightforward to derive that, given $\xi = \frac{\pi}{2} + \tilde{\alpha} + \frac{\phi}{2}$, we have

$$\tilde{d} = d_c \cdot \cos(\xi) + \sqrt{d_c^2 \cdot \cos^2(\xi) - d_c^2 + \tilde{D}^2} \quad (28)$$

The value of \tilde{d} is usually less than that of \tilde{D} . That is, in order to tackle the problem that a moving target may change its direction right after a hand-off, the covering disks of two consecutive duty sensors have to overlap more, and hence the number of duty sensors required will increase. In Section 6.3, we will study the performance impact of using \tilde{d} to determine the relay area.

6 Performance Evaluation and Discussion

In this section we carry out simulation to evaluate the performance of the proposed scheme, with respect to the following metrics:

- (1) The quality of surveillance, M_{QoV} , defined to be the percentage of the target trace covered by duty sensors with pre-specified QoM;

- (2) The number of duty sensors designated by the proposed scheme for target tracking/monitoring.

In the simulation study, n sensors are randomly deployed in a 20×20 area. The $QoM(\alpha, \beta)$ is set to be $\alpha = \beta = 0.05$. The attenuation factor $m = 2$ and the initial power of the target a_0 is set to be 200. The variance of the white noise is set to be $\sigma = 1$. The moving speed in the random waypoint model is set to 1 m/sec, and the pause time is set to zero. Each simulation run lasts for 100 seconds, and all the results presented in this section are the average over 10 runs.

6.1 Quality of Surveillance M_{QoV}

One of the most important aspects of target tracking is the quality of monitoring. In this set of simulation runs, we study whether or not the pre-specified $QoM(\alpha, \beta)$ can be met under the proposed scheme. Fig. 7 depicts M_{QoV} as a function of D , ϕ and w_r , where D is the physical coverage radius of a sensor node.

As shown in Figure 7, as D increases, M_{QoV} decreases. This is because as the physical sensing range D increases, *duty sensors* may be far away from the moving target and hence the sensed signal is attenuated. As a result, likelihood-based detection gives less accurate results. We also observe that the quality of surveillance does not change dramatically with ϕ and w_r . This is in part due to the fact that QoM is determined based on the distance between a target and a duty sensor.

6.2 Number of Duty Sensors Designated for Target Tracking

In this set of simulation runs we study the number of duty sensors designated by the proposed scheme and the time duration that a sensor operates as a *duty sensor*. Fig. 8 gives the number of *duty sensors* as a function of the three parameters. The number of duty sensors decreases as D increases but increases as ϕ increases. The latter is due to that fact that as ϕ increases, it is more likely for the new duty sensor selected to be far away from the moving target direction. As a result, each duty sensor covers less portion of the target trace and more duty sensors are required. The increasing rate is, however, mild, and the impact of ϕ on the number of duty sensors required is not as significant as that of D . Similar observations can be made for w_r .

A comparison between the number of duty sensors designated under the proposed scheme and the bounds derived in Section 4.2 (Eq. (27)) is given in Fig. 9. The number of *duty sensor* required is, in the worst case, approximately 1.2 times larger than the lower bound. This demonstrates the effectiveness of the proposed relay-area based scheme. Fig. 10 gives the average length of the portion of target trace covered by a duty sensor.

Figure 11 gives the time duration during which a sensor is in the tracking mode (and works as a duty sensor). As shown in Fig 11 (a), the time duration fluctuates more dramatically for larger values of D . This is corroborated by the results of the standard deviation of the time duration given in Fig 11 (b). This implies that given a large value of D , it is more likely that some sensors may serve as duty sensors for comparatively longer durations than the others, and hence deplete their energy. In summary, in order to provide a higher M_{QoV} and to ensure load balance among duty sensors, a smaller value of D is preferred. However, the performance with respect to

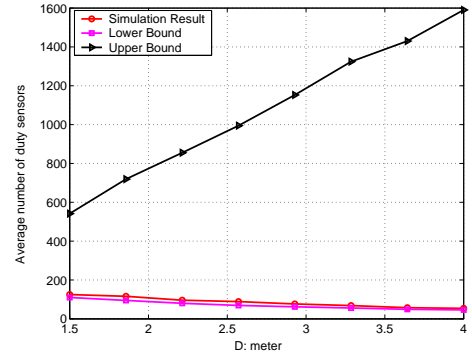


Figure 9. The number of duty sensors designated by the proposed scheme versus the derived lower and upper bounds.

the number of duty sensors argues for a larger value of D . Caution should be exercised to set the value of D so that a trade-off among M_{QoV} , the number of duty sensors required, and the load balance can be achieved.

6.3 Performance of the Modified Hand-Off Scheme

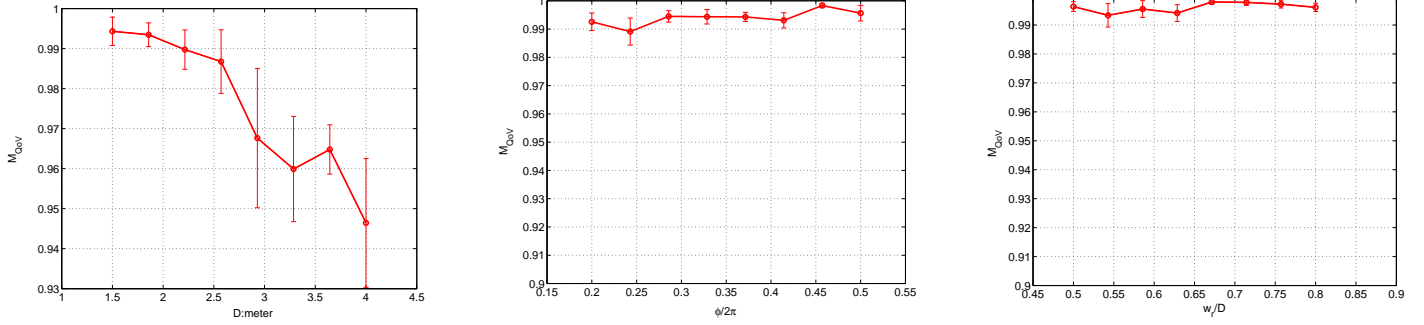
In Section 5.2, in order to provide more coverage of the moving target, we consider the case that the moving direction changes during the process of hand-off. In this section, we study the performance of the refined scheme and compare it with the original one. Since the modified algorithm only changes the distance from P_o to the relay area to \tilde{d} , made in the refined algorithm is that the distance \tilde{d} , we will only consider the parameter D and ignore w_r and ϕ . The experimental setting is the same as above sections and for the modified algorithm, we set $d_c \in [0.1D, 0.2D]$. The experiment results are shown in Fig. 12. In Fig. 12 (a) we show the average number of duty sensors and M_{QoV} is shown in (b). The modified scheme uses more duty sensors and achieves a higher M_{QoV} , which is intuitively correct to the fact that it takes into consideration of the case when the target changes its direction right after it enters the coverage area of a new duty node.

6.4 Performance in the Case That Sensors Are Not Uniformly Distributed

As our derivation is made under the assumption that sensors are uniformly distributed in a field, an interesting question is then whether or not, and to what extent, the performance of the proposed relay-area based scheme degrades when this assumption does not hold. In this subsection, we carry out simulation to study this problem. Specifically, we divide the entire area into 16 blocks. The density in each block is randomly chosen and varies between $[2, 6]$ sensors/ m^2 , and repeat the above experiments.

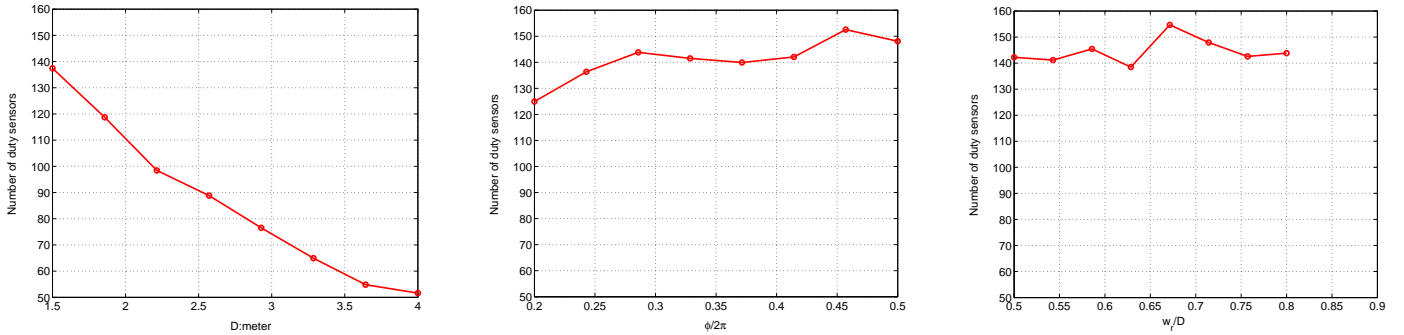
Due to the space limit, we only present the simulation result of the number of duty sensors required under this non-uniform nodal distribution case and compare it with that in the uniform distribution case and the lower bound. As shown in Fig. 13, the number of duty sensors required fluctuates around the lower bound.² Moreover, M_{QoV} degrades from over 99% to approximately 90%. A

²Note that since the lower bound is derived under the assumption of the uniform



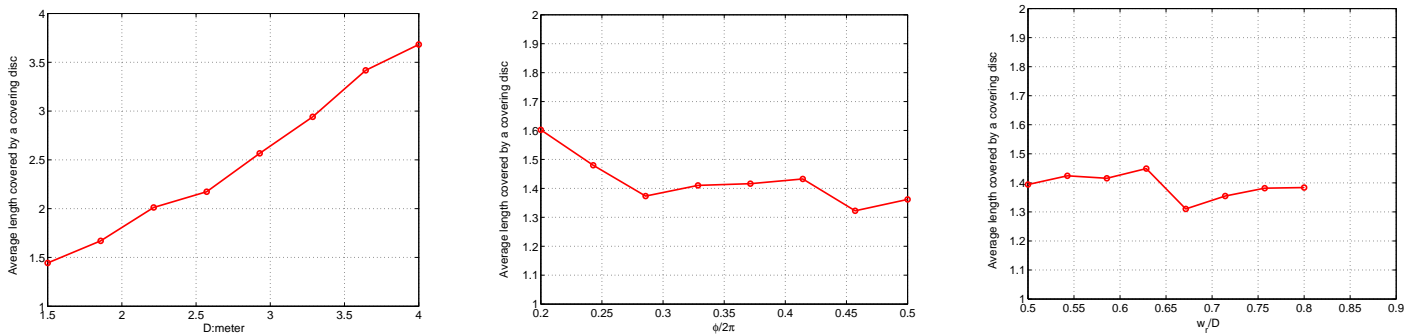
(a) Varying D with $\phi = 2\pi/3, w_r = 2D/3$ (b) Varying ϕ with $D = 1.5m, w_r = 2D/3$ (c) Varying w_r with $D = 1.5m, \phi = 2\pi/3$

Figure 7. The percentage of the target trace that is covered with $QoM(\alpha, \beta)$ as a function of D, ϕ and w_r .



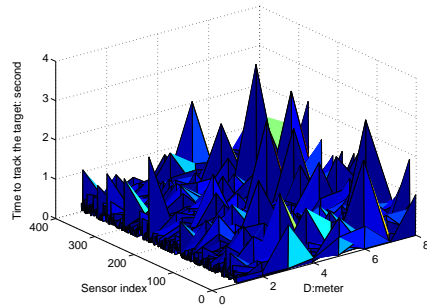
(a) change D with $\phi = 2\pi/3, w_r = 2D/3$ (b) change ϕ with $D = 1.5m, w_r = 2D/3$ (c) change w_r with $D = 1.5m, \phi = 2\pi/3$

Figure 8. The number of sensors designated by the proposed scheme as a function of D, ϕ and w_r .

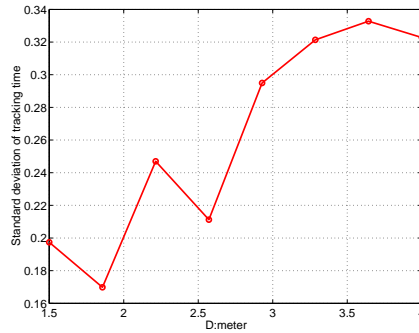


(a) Varying D with $\phi = 2\pi/3, w_r = 2D/3$ (b) Varying ϕ with $D = 1.5m, w_r = 2D/3$ (c) Varying w_r with $D = 1.5m, \phi = 2\pi/3$

Figure 10. The average length of the portion of target trace covered by a duty sensor as a function of D, ϕ and w_r .

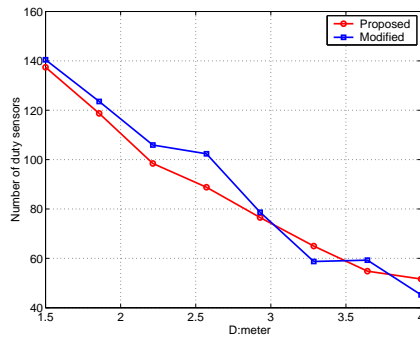


(a) the time duration in the tracking mode

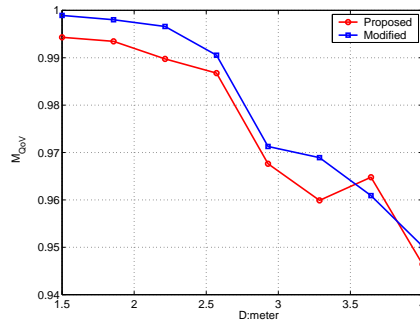


(b) std of the time duration

Figure 11. The duration during which a sensor is in the tracking mode and its std, both versus D .



(a) Number of *duty sensors*



(b) M_{QoV}

Figure 12. Performance comparison between the refined and original hand-off algorithms.

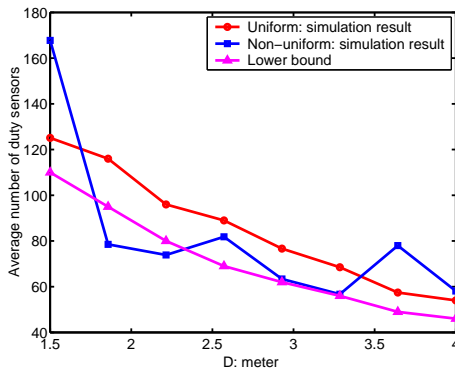


Figure 13. The number of duty sensors designated by the proposed scheme versus the uniform case and the derived lower.

remedy to this degradation is to enable each node to detect the node density in its vicinity and choose the sensing radius accordingly. This is currently under investigation.

nodal distribution, it no longer serves as a lower bound in the non-uniform nodal distribution case. This is why the number of duty sensors required can be smaller than the lower bound in some cases.

7 Conclusion

In this paper, we consider the issue of how to track mobile targets with certain level of *quality of monitoring* (QoM), while conserving power. We address the target tracking problem by taking into account of both the *coverage* and the *QoM*. In particular, QoM gives a certain level of confidence in monitoring a target, i.e., the probability of reporting inaccurate monitoring information (such as false alarm or target miss) should be as small as possible, even in the presence of noises and signal attenuation. We have also studied analytically whether or not the detection/observation made by a single sensor suffices to tracking the target in a reasonably populated sensor network. Our finding gives a confirmative answer and challenges the long-held paradigm that high tracking quality (low tracking error) necessarily requires high power consumption. To rigorously analyze the impact of target movement on QoM, we have derived both lower and upper bounds on the number of sensors (called *duty sensors*) required to keep track of a moving target. Based on the analysis, we have devised a cooperative, *relay-area-based* scheme that determines which sensor should become the next duty sensor when the target is moving.

There are certain limitations of the proposed scheme. In particular, for the sake of determining the relay area, the scheme requires that each sensor node knows its own position, and a localization algorithm has to be included. This may increase both the computational and communication overhead. How to relax this requirement by devising a lightweight method to determine the relay area is currently under investigation. Also, we are investigating the issue of

enabling each node to detect the node density in its vicinity (so that an appropriate sensing radius can be determined to ensure QoM) in the case of non-uniform nodal distributions.

References

- [1] I. Akyildiz, W. Sun, Y. Sankarasubramaniam, and E. Cayirci. A Survey on Sensor Networks. *IEEE Communications Magazine*, Vol. 40, No. 8, pp.102-114, August 2002.
- [2] J. Aslam, Z. Bulter, V. Crespi, G. Cybenko, and D. Rus. Tracking a moving object with a binary sensor network. In *ACM International Conference on Embedded Networked Sensor Systems (SenSys)*, 2003.
- [3] J. Broch, D.A. Maltz, D.B. Johnson, Y.C. Hu, and J. Jetcheva. A performance comparison of multi-hop wireless ad hoc network routing protocols. In *Proc. ACM Intern. Conf. on Mobile Computing and Networking (Mobicom'98)*, Dallas, TX, October 1998.
- [4] M. Cardei, and J. Wu. *Handbook of Sensor Networks*, chapter Coverage in Wireless Sensor networks. CRC Press, 2004.
- [5] A. Cerpa *et al.* Habitat monitoring: Application driver for wireless communications technology. In *2001 ACM SIGCOMM Workshop on Data Communications in Latin America and Caribbean*, Costa Rica, April 2001.
- [6] A. Cerpa and D. Estrin. ASCENT: Adaptive self-configuring sensor networks topologies. In *Proc. of INFOCOM 2002*, March 2002.
- [7] K. Chakrabarty, S. S. Iyengar, H. Qi and E. Cho. Grid coverage for surveillance and target location in distributed sensor networks. *IEEE Transaction on Computers*, 51(12), 2002.
- [8] W.-P. Chen, J. C. Hou, and L. Sha, "Dynamic clustering for acoustic target tracking in wireless sensor networks," *IEEE Trans. on Mobile Computing*, special issue on *Mission-oriented sensor networks*, Vol. 3, Number 3, July-September 2004.
- [9] B. Chen, K. Jamieson, H. Balakrishnan, and R. Morris. Span: An energy-efficient operation in multihop wireless ad hoc networks. In *Proc. of ACM MobiCom'01*, 2001.
- [10] M. Chu, H. Haussecker, and F. Zhao. Scalable information-driven sensor querying and routing for ad hoc heterogeneous sensor networks. *International Journal on High Performance Computing Applications*, 16(3), 2002.
- [11] D. Estrin *et al.* Embedded, Everywhere: A Research Agenda for Networked Systems of Embedded Computers. National Research Council Report, 2001.
- [12] C. Gui and P. Mohapatra. Power Conservation and Quality of Surveillance in Target Tracking Sensor Networks. In *ACM/IEEE International Conference on Mobile Computing and Networks (MobiCom '04)*, Philadelphia, PA, September, 2004.
- [13] P. Hall. *Introduction to the Theory of Coverage Process*. John Wiley and Sons, Inc., 1988.
- [14] T. He, C. Huang, B. M. Blum, J. A. Stankovic, and T. Abdelzaher, "Range-free localization schemes for large scale sensor networks," in *Proc. ACM International Conference on Mobile Computing and Networking (MOBICOM)*, San Diego, CA, USA, Sept. 2003, pp. 81–95.
- [15] C. F. Huang and Y. C. Tseng. The coverage problem in a wireless sensor network. In *ACM Workshop on Wireless Sensor Networks and Applications (WSNA)*, 2003.
- [16] K. Mechitov, S. Sundresh, Y. Kwon, and G. Agha. Cooperative tracking with binary-detection sensor networks. Technical Report UIUCDCS-R-2003-2379, Computer Science Dept., University of Illinois at Urbana-Champaign, 2003.
- [17] S. Patten, S. Poduri and B. Krishnamachari. Energy-Quality Tradeoffs for Target Tracking in Wireless Sensor Networks. *2nd Workshop on Information Processing in Sensor Networks, IPSN*, April 2003.
- [18] G.J. Pottie, W.J. Kaiser. Wireless Integrated Network Sensors. *Communications of ACM*, Vol. 43, No. 5, pp.551-558, May 2000.
- [19] E.M. Royer and C.E. Perkins. Multicast operation of the ad-hoc on-demand distance vector routing protocol. In *Proc. ACM Intern. Conf. on Mobile Computing and Networking (Mobicom'99)*, Seattle, WA, August 1999.
- [20] S. Shakkottai, R. Srikant, and N. B. Shroff. Unreliable sensor grids: Coverage, connectivity and diameter. In *Proc. of IEEE INFOCOM*, pp. 1073-1083, San Francisco, CA, 2003.
- [21] S. Slijepcevic and M. Potkonjak. Power efficient organization of wireless sensor networks. In *IEEE International Conference on Communication*, 2001.
- [22] P. Varshney. *Distributed Detection and Data Fusion*. Springer-Verlag, New York, NY, 1996.
- [23] Q.X. Wang, W.P. Chen, R. Zheng, K. Lee, and L. Sha. Acoustic target tracking using tiny wireless sensor devices. In *International Workshop on Information Processing in Sensor Networks (IPSN)*, 2003.
- [24] X. Wang, G. Xing, Y. Zhang, C. Lu, R. Pless, and C. Gill. Integrated coverage and connectivity configuration in wireless sensor networks. In *ACM Sensys'03*, Nov. 2003.
- [25] J. Warrior. Smart Sensor Networks of the Future. *Sensors Magazine*, March 1997.
- [26] H. Yang and B. Sikdar. A protocol for tracking mobile targets using sensor networks. In *IEEE International Workshop on Sensor Networks Protocols and Applications*, 2003.
- [27] F. Ye, G. Zhong, S. Lu, and L. Zhang. Energy efficient robust sensing coverage in large sensor networks. Technical report, UCLA, 2002.
- [28] F. Ye, G. Zhong, S. Lu, and L. Zhang. Peas: A robust energy conserving protocol for long-lived sensor networks. In *The 23rd International Conference on Distributed Computing Systems (ICDCS)*, 2003.

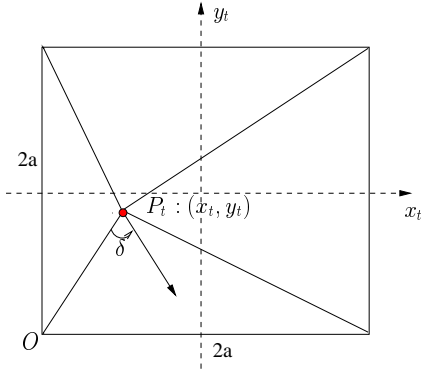


Figure 14. The definition of δ in a $2a \times 2a$ area.

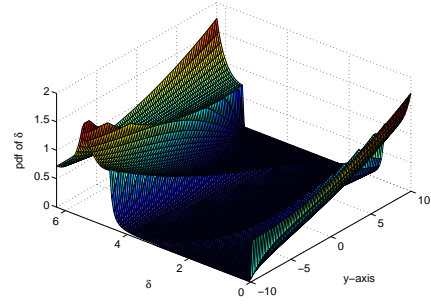


Figure 15. The pdf of θ when $x_t = 7$ and $y_t \in [-10, 10]$.

the lower bound on the number of duty sensors required (derived in Section 4.1).

- [29] H. Zhang and J. C. Hou, “Maintaining sensing coverage and connectivity in large sensor networks,” *Wireless Ad Hoc and Sensor Networks: An International Journal*, Vol. 1, No. 1, January 2005.
- [30] W. Zhang and G. Cao. DCTC: Dynamic convoy tree-based collaboration for target tracking in sensor networks. *IEEE Trans. on Wireless Communications*, 2004.
- [31] W. Zhang and G. Cao. Optimizing tree reconfiguration for mobile target tracking in sensor networks. In *IEEE INFOCOM*, 2004.
- [32] F. Zhao, J. Shin, and J. Reich. Information-driven dynamic sensor collaboration for tracking applications. *IEEE Signal Processing Magazine*, March 2002.

A Direction of sensor nodes in a grid

Since the direction taken by a target affects the length of the chord, we derive the probability density function (pdf) of the direction of the moving target. Consider a $2a \times 2a$ area. The target is initially located at $P_t = (x_t, y_t)$, randomly picks a destination, and travels toward that destination at a constant speed. As shown in Fig. 14, let δ denote the angle between the line $\overline{OP_t}$ and the moving direction.

By defining $\delta_1 = \pi - \arctan(\frac{y_t+a}{x_t+a}) - \arctan(\frac{y_t+a}{x_t+a})$, $\delta_2 = \pi - \arctan(\frac{a-x_t}{a+y_t}) - \arctan(\frac{a-x_t}{a-y_t}) + \delta_1$, $\delta_3 = \pi - \arctan(\frac{a-y_t}{a-x_t}) - \arctan(\frac{a-y_t}{a+x_t}) + \delta_2$, $\delta_4 = 2\pi$, it is straightforward to derive the pdf of δ as

$$f(\delta|x_t, y_t) = \begin{cases} \frac{(a+y_t)^2(1+\tan^{-2}(\eta+\delta))}{2a^2}, & \text{if } 0 \leq \delta < \delta_1, \\ \frac{(a-x_t)^2(1+\tan^2(\eta+\delta))}{2a^2}, & \text{if } \delta_1 \leq \delta < \delta_2, \\ \frac{(a-y_t)^2(1+\tan^{-2}(\eta+\delta))}{2a^2}, & \text{if } \delta_2 \leq \delta < \delta_3, \\ \frac{(a+x_t)^2(1+\tan^2(\eta+\delta))}{2a^2}, & \text{if } \delta_3 \leq \delta \leq 2\pi, \end{cases} \quad (29)$$

where $\eta = \arctan(\frac{a+y_t}{a+x_t})$. Fig. 15 depicts the pdf of δ when $a = 10$. Note that the pdf changes with three variables (δ , x_t , and y_t), and what is shown in Fig. 15 is the results when $x_t = 7$ and $y_t \in [-10, 10]$. An important finding from the figure is that under the random waypoint model, the direction toward which the target moves in the next epoch is *not* uniformly distributed. Instead, it depends on its current location. Due to this property, we will refine